AGU PUBLICATIONS

Geochemistry, Geophysics, Geosystems

RESEARCH ARTICLE
10.1002/2013GC005164

Special Section:
The Lithosphere-asthenosphere System

Crustal thickness and velocity structure across the Moroccan Atlas from long offset wide-angle reflection seismic data: The SIMA experiment

P. Ayarza[1], R. Carbonell[2], A. Teixell[3], I. Palomeras[4], D. Martí[2], A. Kchikach[5], M. Harnafi[6], A. Levander[4], J. Gallart[2], M. L. Arboleya[3], J. Alcalde[2], M. Fernández[2], M. Charroud[7], and M. Amrhar[5]

[1]Departamento de Geología, Universidad de Salamanca, Salamanca, Spain, [2]Instituto de Ciencias de la Tierra, "Jaume Almera", CSIC, Barcelona, Spain, [3]Departament de Geologia, Universitat Autònoma de Barcelona, Bellaterra, Spain, [4]Department of Earth Sciences, Rice University, Houston, Texas, USA, [5]Faculté des Sciences et Techniques, Semlalia, Université Cadi-Ayyad, Marrakech, Morocco, [6]Institut Scientifique, Agdal, Rabat, Morocco, [7]Faculté des Sciences et Techniques, Université Sidi Mohammed Ben Abedellah, Fes, Morocco

Abstract The crustal structure and topography of the Moho boundary beneath the Atlas Mountains of Morocco has been constrained by a controlled source, wide-angle seismic reflection transect: the SIMA experiment. This paper presents the first results of this project, consisting of an almost 700 km long, high-resolution seismic profile acquired from the Sahara craton across the High and the Middle Atlas and the Rif Mountains. The interpretation of this seismic data set is based on forward modeling by raytracing, and has resulted in a detailed crustal structure and velocity model for the Atlas Mountains. Results indicate that the High Atlas features a moderate crustal thickness, with the Moho located at a minimum depth of 35 km to the S and at around 31 km to the N, in the Middle Atlas. Upper crustal shortening is resolved at depth through a crustal root where the Saharan crust underthrusts the northern Moroccan crust. This feature defines a lower crust imbrication that, locally, places the Moho boundary at ~40–41 km depth in the northern part of the High Atlas. The P-wave velocity model is characterized by relatively low velocities, mostly in the lower crust and upper mantle, when compared to other active orogens and continental regions. These low deep crustal velocities together with other geophysical observables such as conductivity estimates derived from MT measurements, moderate Bouguer gravity anomaly, high heat flow, and surface exposures of recent alkaline volcanism lead to a model where partial melts are currently emplaced at deep crustal levels and in the upper mantle. The resulting model supports the existence of a mantle upwelling as mechanism that would contribute significantly to sustain the High Atlas topography. However, the detailed Moho geometry deduced in this work should lead to a revision of the exact geometry and position of this mantle feature and will require new modeling efforts.

Key Points:
- A crustal-scale imbrication has been identified in the Moroccan Atlas Mountains
- Very low P-wave velocities in the lower crust and mantle of the Moroccan Atlas
- The new Moho depth implies slight modifications to the LAB depth

Correspondence to:
P. Ayarza,
puy@usal.es

Citation:
Ayarza, P., et al. (2014), Crustal thickness and velocity structure across the Moroccan Atlas from long offset wide-angle reflection seismic data: The SIMA experiment, *Geochem. Geophys. Geosyst.*, *15*, 1698–1717, doi:10.1002/2013GC005164.

Received 21 NOV 2013
Accepted 1 MAR 2014
Accepted article online 5 MAR 2014
Published online 7 MAY 2014

1. Introduction

Long offset wide-angle seismic reflection experiments have proven to be a useful tool in the determination of the crustal thickness and structure [*Prodehl and Mooney*, 2012]. In these type of data, the high-velocity contrast between the deep crust and the mantle benefits from the increase of the reflection coefficients at offsets above the critical distance, and supplies high-amplitude phases that are the key to model the geometry and depth of the Moho boundary [*Carbonell et al*., 1996, 2000; *Palomeras et al*., 2009]. In addition, when densely sampled, this type of data set provides accurate constraints on the velocity structure of the area under investigation and is one of the keys to resolve crustal or lithospheric composition, rheology, and occasionally, internal structure [*Flecha et al*., 2009; *Palomeras et al*., 2011].

Knowledge of the geometry and depth to the Moho boundary is important to understand the evolution of orogenic belts. Processes like late-orogenic re-equilibration, isostasy, magmatism, etc. leave their imprints on the crust-mantle boundary position and structure. Thus, these features often become crucial to study the development of deep seated processes that can only be partly inferred through the study of surface geology.

The Moroccan Atlas Mountains have been a target of scientific research in the last decades [*Frizon de Lamotte et al*., 2008; *Teixell et al*., 2007]; the origin of their high topography in a context of limited orogenic

deformation, together with the existence of an intriguing alkaline volcanism, intermediate depth seismicity, and high heat flow have been major subjects of study. Geological and geophysical features of the Atlas region led geologists to assume that the Atlas crust is thin and thus, its topography is not totally supported by local isostasy but aided by some sort of mantle upwelling (see review in *Teixell et al*., [2003]). Accordingly, potential-field lithospheric models (based on free-air and Bouguer gravity anomalies and geoid undulations) have placed the lithosphere/asthenosphere boundary (LAB) at anomalously shallow depths underneath the central Moroccan Atlas [*Teixell et al*., 2005; *Zeyen et al*., 2005]. These models, however, rely on estimations of crustal thickness made on the basis of (a) gravity data [*Ayarza et al*., 2005] that regardless of being well constrained by surface geology, may offer multiple solutions, (b) local receiver functions, that only provide 1-D information [*Sandvol et al*., 1998; *Van der Meijde et al*., 2003], and (c) old, low-resolution, wide-angle data [*Tadili et al*., 1986; *Wigger et al*., 1992]. From an isostatic point of view, it is obvious that a crust thicker than that included in the lithospheric models would deepen the LAB and vice versa.

In order to better constrain the High and Middle Atlas crustal thickness, its rheology at a deep level, its overall structure and, subsequently, the depth of the LAB, the SIMA (Seismic Imaging of the Moroccan Atlas) project aimed to the acquisition of a wide-angle reflection seismic line in spring of 2010. Here we present the first results of the modeling and interpretation of the SIMA profile, addressing the number and position of crustal interfaces, the geometry of the Moho boundary, and the velocity structure. Finally, we review the implications that these results have on the validity of the lithospheric models presented up to date and on the understanding of the geodynamics of the Atlas orogenic belts.

2. Geological and Geophysical Setting

The Atlas Mountains is a ~2000 km long intracontinental orogenic belt located in northern Africa, near the boundary between the African and Euroasiatic plates. Its westernmost branches, the High and Middle Atlas of Morocco (Figure 1), correspond to Mesozoic extensional basins related to the opening of the Atlantic and Tethys oceans [*Arboleya et al*., 2004; *Beauchamp et al*., 1999; *Frizon de Lamotte et al*., 2000; *Gómez et al*., 2000; *Laville and Piqué*, 1992; *Mattauer et al*., 1977; *Teixell et al*., 2003], and later inverted as a consequence of the Cenozoic-to-present convergence between Eurasia and Africa [*Laville et al*., 1977; *Medina and Cherkaoui*, 1991; *Morel et al*., 2000, 1993].

In the High and the Middle Atlas, orogenic contraction was mainly achieved by thick-skinned thrusting and folding affecting the pre-Mesozoic basement and the Mesozoic–Cenozoic cover. Thin-skinned thrusting usually played a minor role and appears related to basement underthrusting [*Teixell et al*., 2003]. According to these authors, the total shortening due to Cenozoic compression in the central High Atlas varies between 15% in the west to 24% to the east, and keeps an inverse relationship with altitude, which in the west reaches 4000 m. The Middle Atlas has also a simple structure: variations in the structural elevation of the Mesozoic beds suggest that basement is involved in the deformation, and shortening is below 10% [*Arboleya et al*., 2004].

The Moroccan Atlas also hosts Cenozoic to Quaternary alkaline to peralkaline magmatism, synchronous with compression [*Harmand and Cantagrel*, 1984]. Geochemical data obtained from Quaternary lavas indicate the existence of a depleted asthenosphere that interacted with the mantle lithosphere [*El Azzouzi et al*., 1999]. This magmatism has similar petrology and signature to that of the Canary Islands and accordingly, a common source for both of them has been proposed [*Anguita and Hernan*, 2000].

P-wave velocity anomalies have been identified underneath the Atlas Mountains. A thin and/or anomalously hot lithosphere and upper mantle has been proposed on the basis of low P-wave velocities [*Seber et al*., 1996] that seems to extend to a large part of NW Africa and to western Europe [*Bijwaard and Spakman*, 2000; *Hoernle et al*., 1995]. Relatively high heat flow values occurring in Morocco, ranging between 40 and 100 mWm^{-2} [*Rimi*, 1999], are in agreement with these observations. Although a high heat flow does not necessarily represent a hot mantle, a 50 km thick lithosphere was proposed by *Ramdani* [1998] to explain values of 86 mWm^{-2} in the southern High Atlas.

The first estimations of the thickness of the Atlas crust were obtained from low-resolution refraction and wide-angle reflection data acquired in the 1970s [*Tadili et al*., 1986]. These authors present Moho depths of 40 km for the central part of the High Atlas and 38 km to the east. Yet another seismic experiment, partly

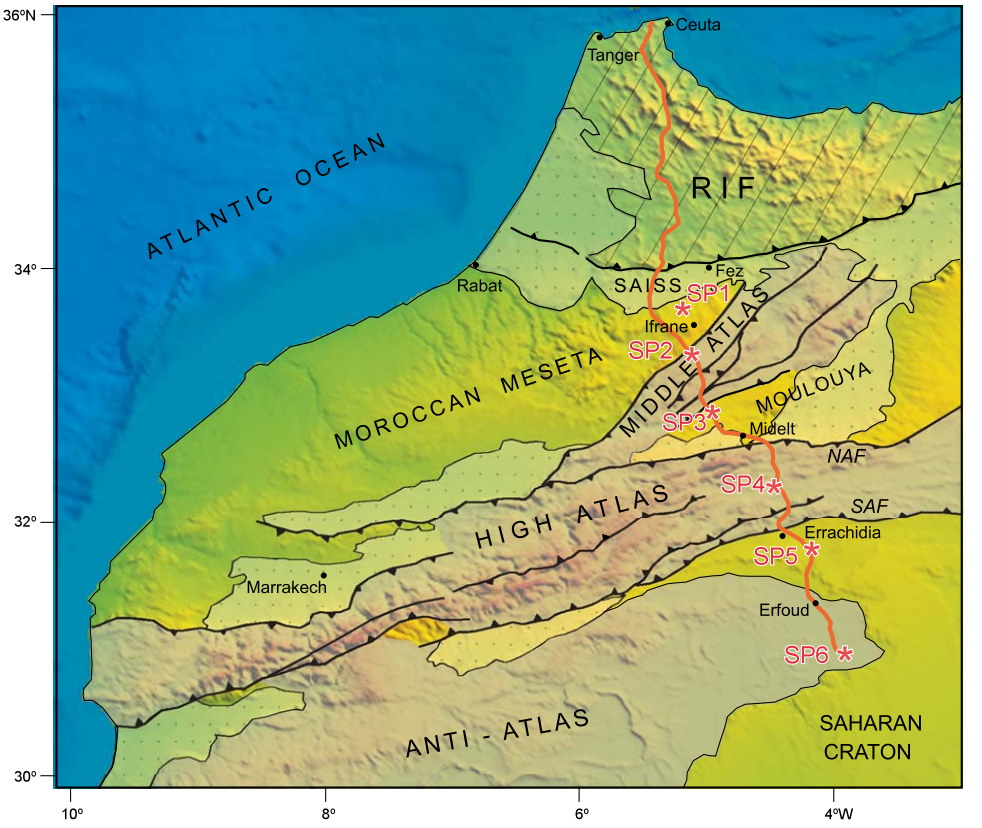

Figure 1. Tectonic sketch of the Atlas and Rif Mountains over a digital elevation model of Morocco, showing shot point locations and recording stations of the SIMA experiment. SP#: Shot Point number; SAF: South Atlas Fault; NAF: North Atlas Fault; Orange line: location of the recording stations.

coincident with the transect presented here, was carried out in 1986 [*Giese and Jacobshagen*, 1992; *Wigger et al*., 1992]. The results propose a relatively thin crust underneath the High Atlas (38–39 km) that becomes even thinner to the N and S (35 km), thus defining a crustal root about 3–5 km deep. These models also show low P-wave velocities for the crust, which appears highly differentiated, and for the upper mantle. Several low velocity zones were modeled in the crust: a shallow one located at 10–15 km depth and coincident with a layer of high conductivity [*Schwarz et al*., 1992] was interpreted as a basal fault detachment. Another low velocity zone found in the lower crust was attributed to melt relics from the Mesozoic rifting.

Bouguer gravity anomaly data have been modeled along two transects that cross the eastern and central High Atlas [*Ayarza et al*., 2005], the former being coincident with part of the seismic profile here presented. These authors use surface geology and receiver functions data to constrain the depth and geometry of the different boundaries and divide the Atlas crust in three layers, namely sediments, upper crust, and lower crust. In the easternmost section, the Moho seems to be deepest to the north of the peak altitudes of the High Atlas, thus evidencing the relative mismatch between the Bouguer anomaly data and the topography, which is also manifested in a general positive isostatic anomaly.

A magnetotelluric (MT) survey coincident with *Wigger et al*.'s [1992] seismic experiment pointed out the existence of a north-dipping high-conductivity zone starting near the surface in the southern border of the High Atlas and either flattening down at midcrustal levels or dipping continuously northward down to lower crustal depths [*Schwarz et al*., 1992]. More recent MT surveys have found evidence of a conductive lower crust underneath the Moulouya plain (see location in Figure 1), which together with other data, led the authors to infer the existence of a fraction of 2–8% of partial melt near the Atlas crustal root, at 30–35 km depth [*Ledo et al*., 2011]. Finally, on the basis of a similar long period MT survey, a conductive anomaly located at 40 km has been interpreted as melting at the top of an anomalous mantle in connection with the Middle Atlas quaternary basaltic volcanism [*Anahnah et al*., 2011].

Potential field-based lithospheric models, running from SW Iberia to the Sahara desert, have taken into account most of the observations above described and have concluded that the Atlas topography is supported by some sort of mantle upwelling that places the asthenosphere at ~70 km under the Atlas Mountains [*Fullea et al*., 2010; *Teixell et al*., 2005; *Zeyen et al*., 2005]. This plume-like feature has also an influence on the elevation of the Anti-Atlas, the Maroccan Meseta and the bordering high-altitude plains, as well as in the alkaline volcanism of the region. Regardless of the origin of this anomaly, the exact depth of the risen LAB boundary depends greatly on the long wave-length topography of the Moho, which up to now, was only constrained by low-resolution wide-angle seismic [*Tadili et al*., 1986; *Wigger et al*., 1992] and gravity data [*Ayarza et al*., 2005].

Currently, a large amount of passive seismic data are being acquired across the plate boundary between northern Africa and southern Iberia by international collaboration projects, like TOPOIBERIA and PICASSO, and are coming up with relatively high-resolution large-scale tomography models for the area. These models find outstanding differences in the velocity structure of northern Africa, with velocities (Vs) lower than the average underneath the Atlas Mountains [*Palomeras et al*., 2013].

3. The SIMA Experiment

With the goal of constraining the exact crustal thickness and the overall structure of the Atlas Mountains, a high-resolution controlled-source wide-angle reflection seismic experiment was carried out in Morocco in spring 2010. The energy released by six explosions was recorded by 939 Reftek 125a stations (Texans) from the IRIS instrument pool (Figure 1). Stations were deployed between Tanger and the Sahara desert, with an average spacing of 400 m from the S of Fes to Merzouga and of ~1000 m from Fes to Tanger, making resolution more than twice as high in the southern part of surveyed area. The location of the shots did not cover the entire length of the profile, the first one being placed north of the Middle Atlas and the last one S of Merzouga, in the gates of the Sahara desert (Figure 1), with an average spacing of 70 km between them. The charge (approximately 1 TM) was distributed in 2–4 boreholes per shot point at depths of 30–60 m. The quality of the data is best in the central part of the profile, in the area sampling the Middle and High Atlas, and decreases to the S and mostly to the N, where very little information was obtained to the N of the Saiss Basin (Figure 1).

3.1. Shot Gathers

As a result of the experiment, we obtained six shot sections with a reasonable signal to noise (S/N) ratio. Processing steps included the standard for this type of data: application of a reduction velocity (6 and 8 km/s), band-pass filtering (0.5, 1, 12, and 18 Hz: low and high cut-off frequencies of 1 and 12 Hz, respectively), and equalization. Also, deconvolution plus another pass of frequency filtering were applied to eliminate reverberations. Lower frequency filters were also applied in order to improve the continuity for the deep seismic phases. However, these efforts did not result in better resolved sections as some of the shallow phases lost resolution. The obtained seismic sections, reduced at Vred = 8 km/s, is presented together with the surface topography in Figure 2.

The altitude changes along the profile imply that some stations are located almost at sea level whereas others lie at >2000 m. This fact hinders the straightforward interpretation of long, linear phases, and often impedes the correlation of energy along high offsets. Nevertheless, most shot gathers allow the identification of 4–5 phases which have been named in relation to their offsets/travel time, following the standard nomenclature for this type of data set. These are Ps, Pg, PiP, PmP, and Pn and will be described next for every shot gather.

Shot 1, located near Boufekrane, to the N of the Middle Atlas (Figure 1), allows the identification of five phases (Figure 2a). Ps shows low velocities, well below 6 km/s and appears only to the S of the shot and along near offsets (<20 km). Pg appears as a clear phase to the S of the shot, being the first arrival up to distances of 80 km. It shows abrupt changes in travel time probably related to varying elevation. To the N, Pg appears as a much weaker linear phase, and can only be followed up to 40 km. Changes in the character (reflectivity and travel time) of this phase between 50 and 110 km coincide with the low topography of the Saiss Basin (Figure 1) and are preliminarily linked to its low velocity sedimentary infill. A weak and short phase named PiP appears to the S of the shot point at offsets between 50 and 120 km. This phase is not observed to the N of the shot point. A phase labeled PmP appears showing high amplitudes at around 80 km to the S (critical

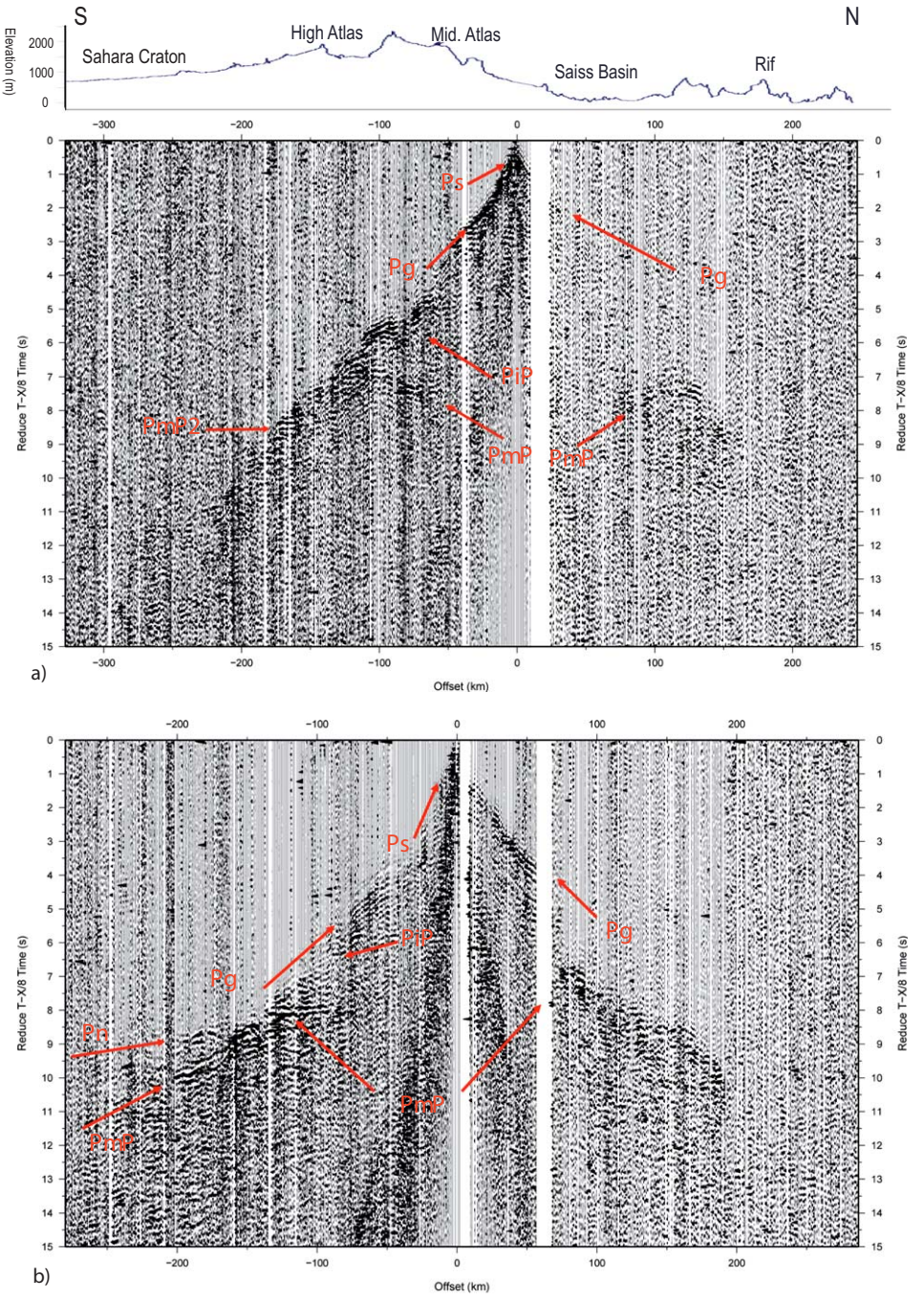

Figure 2. Record sections of shots 1 to 6, numbered from Figures 2a to 2f according to the position of the shot point from N to S (Figure 1). Reduction velocity (Vred) is 8 km/s. Seismic phases are identified (see text for explanation).

distance). To the N, this phase is weaker and shows maximum amplitudes at offsets slightly below 100 km. Finally, a phase is observed from 125 km to the S. Its moveout is almost parallel to that of PmP and it has been named PmP2. Shot gathers plotted at Vred = 8 km/s (Figure 2) allow us to easily estimate the time and critical distance differences (if any) between the N and S branches of the PmP. Note that, for this section, both branches of the PmP arrive at similar times and have maximum amplitudes at similar offsets (7.5 s at 100 km). This indicates that the interface that originates them (the Moho) is fairly horizontal between the reflection points. A linear short phase dipping toward far offsets is identified to the N of the shot point at distances of 100–150 km when reduced at 6 km/s. This phase has been identified as Pn.

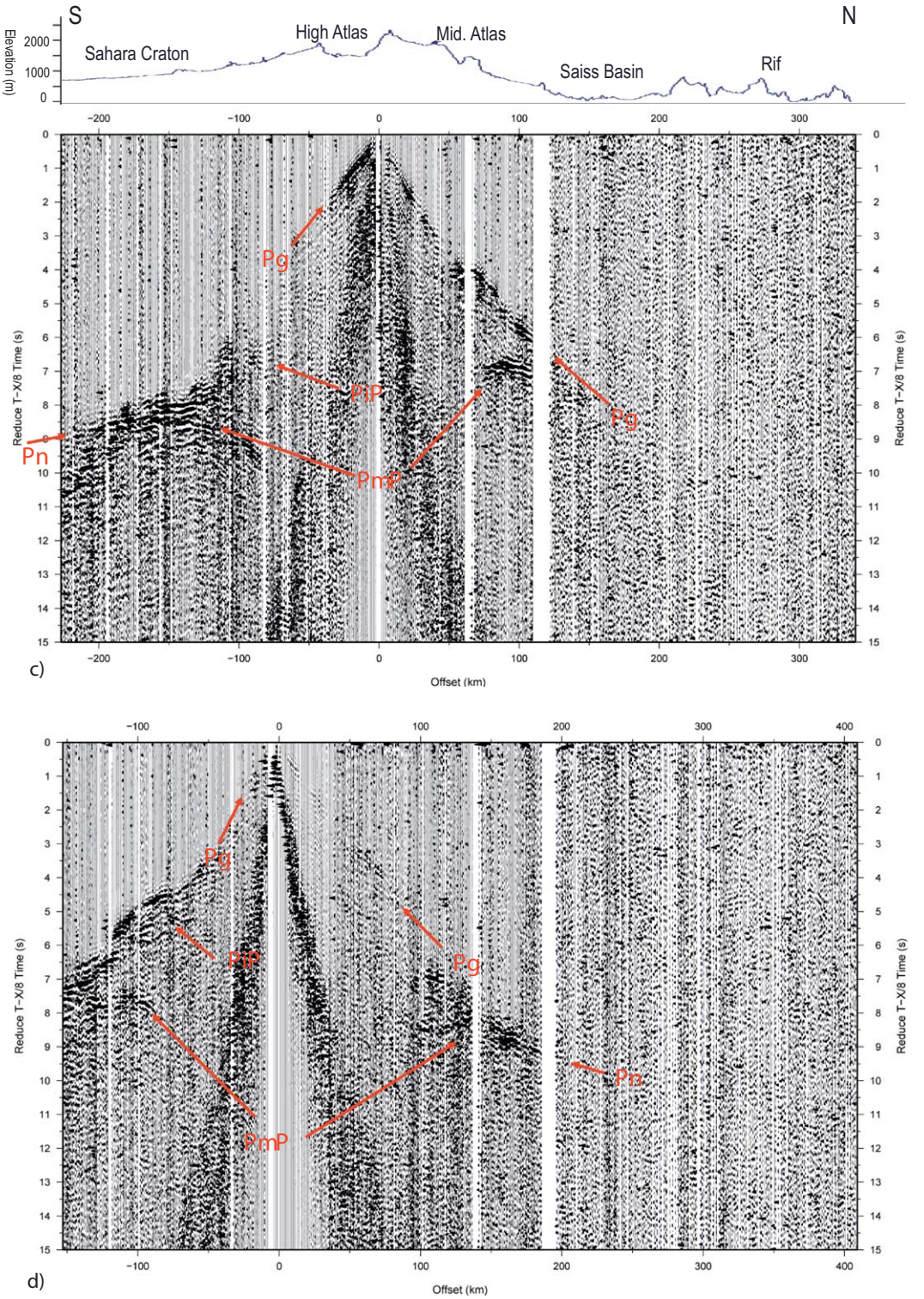

Figure 2. (Continued).

Shot 2, located near Jebel Habri, in the Middle Atlas (Figure 1), allows the identification of five phases (Figures 2b). Ps is observed to the S of the shot gather along a distance of 30 km. This phase is overtaken by Pg, which seems to be first arrival up to distances of >100 km. To the N, this phase is also first arrival along ~50 km and probably more, but severely decreases its amplitude at 70 km, again coinciding with the location of

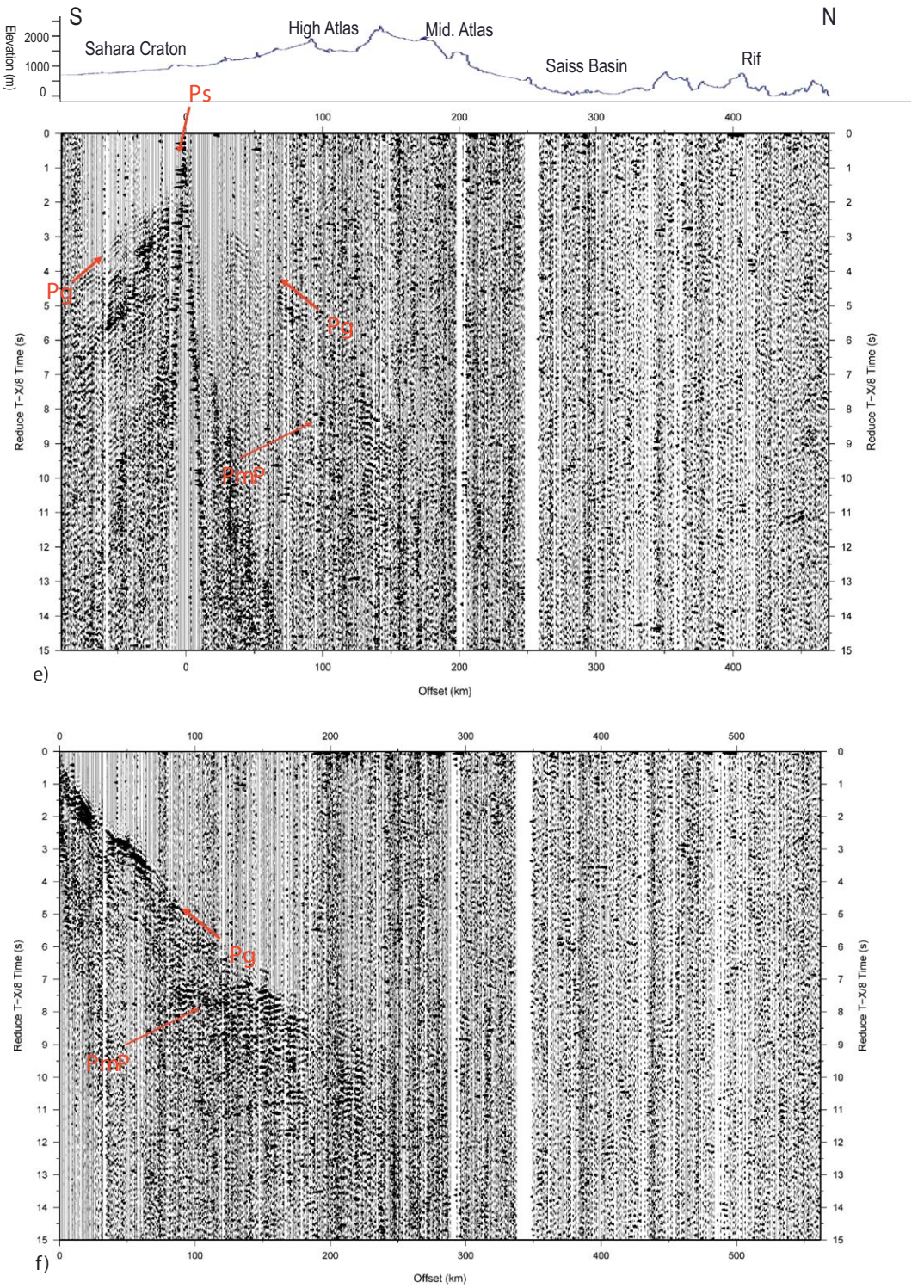

Figure 2. (Continued).

the Saiss sedimentary basin. A PiP phase appears over the distance range of 70–110 km to the S of the shot. The PmP phase appears to the N and S of the shot point at approximate critical distances of 100 and 110 km, respectively, and travel times that are slightly higher for the southern branch (7.1 s to the N versus 7.5 s to the S, with a Vred = 8 km/s, Figure 2b). Also, this phase shows considerable higher amplitudes to the S than to the N of the shot point. A Pn phase is observed to the S, departing from the PmP critical distance to almost the southern end of the profile. This phase is better observed with a Vred = 6 km/s and does not appear to the N of the shot point. This record section stands out due to the high amplitudes and number of reflective events that appear between the PmP and the Pn to the S of the shot point.

Shot 3 was located near Zaida, in the Moulouya Plain, to the N of the High Atlas (Figure 1). In this shot record, four phases can be identified (Figure 2c), the first of them being Pg, which appears as a first arrival up to 100 km to the S and 110 to the N. A PiP phase can be observed to the S, at offsets between 80 and 120 km. This phase is taken over by PmP, which shows critical distances of approximately 140 km. This clearly contrasts with the critical distances at which PmP is observed in shots 1 and 2, and also, in the northern part of this shot gather, where a very well defined PmP shows its higher amplitudes at >100 km. In addition, the time at which we observe the PmP critical arrivals to the N is below 7 s whereas to the S, it is above 8 s, suggesting a clear asymmetry in the crustal thickness and/or velocity structure at both sides of this shot point. Also, to the S, this phase appears to have very high moveout, which can be indicative of a dipping interface or diffractions.

Shot 4, located near Rich, in the High Atlas (Figure 1), shows also four identifiable phases, Pg, PiP, PmP, and Pn (Figures 2d). Pg appears as first arrival to the S up to a distance close to 100 km, where it merges PiP. To the N, it also continues as first arrival up to ~100 km, although, in places, it has low to moderated amplitudes. PmP appears at high critical distances (130 km to the N and 105–120 km to the S) when compared to shots 1 and 2, and slightly lower than in the southern part of shot 3. A short Pn can be observed as a first arrival to the N, at distances over 160 km. To the N of this distance, no phases can be observed since reflectivity decreases dramatically.

Shot 5, located in Tydrine, near Erfoud (Figure 1) shows little reflectivity and only three phases can be identified with certainty (Figure 2e). Ps is observed to the S of the shot point along very short offsets and exhibiting a very low apparent velocity. Pg appears to the N and S of the shot point showing a very reverberative character, mostly to the N. Also to the N, some indications exist of a short PmP phase, arriving at critical distances of 110–120 km. The lack of coherent and long deep identifiable phases in this shot gather is tentatively related with the low density, high porosity Cretaceous beds exposed at the surface where the shot was located.

Shot 6, to the S of Merzouga (Figure 1), represents the southernmost shot point of the experiment and the only one with an end-on geometry. Unfortunately, this shot gather shows also little reflectivity and only Pg and PmP/Pn phases can be observed. Pg appears as first arrival along almost 150 km. It is not clear though if it merges some intracrustal phase at >100 km. PmP can be observed from 100–105 km to 160 km. The existence of a Pn phase is not clear although some hints are observed when reduced at 6 km/s.

3.2. Interpretation

The interpretation of the SIMA data set has been carried out through forward modeling using the "Rayinvr" ray-tracing-based utilities [*Zelt and Smith*, 1992]. This code uses a simple parameterization and is valid for the Middle and especially for the High Atlas, whose structural grain is subperpendicular to the seismic line. A reference line has been defined which allows the projection of source and receivers preserving the original offsets. Since the processing of the data does not include static corrections, we have entered the elevation of the stations in the model every 10 km (i.e., every 20 stations in the S and every 10 stations in the N). We have departed from a simple 2-D, P-wave velocity structure and we have iteratively modified the position of the interfaces and velocities until the observed and the modeled travel times present a good fit. A simple layer stripping approach was followed. Shallow/early arrivals (travel time picks) were used to constrain the velocity of the shallowest part of the model. Later phases were then included progressively, in order to define a crust and upper mantle model. Because of the complexity of the data and arrivals, models were obtained using a trial and error methodology for each shot and then combined into a single model that accounts for all arrivals. Even though interpretations based on forward modeling are geared toward

layer-cake velocity models, densely spaced recordings increase the resolution of the data and allow the inclusion of heterogeneities that witness the complexities existing in the crust.

Since one of the main goals of the SIMA experiment was to map the crust-mantle boundary as exactly as possible, special attention has been paid to offsets and travel times of PmP and Pn phases. Whereas shot gathers 1 and 2 show PmP critical distances of ~100 km to the N and S of the shot points, shot number 3 features, for the same phase, critical distances of >140 km to the S and 100 km to the N (Figure 2c), thus providing us with key information to understand the crustal structure of the Atlas. Finally, shots 4, 5, and 6, show PmP critical distances higher than 100 km but often well below 140 km. Together with these variations in the critical distance, the PmP phase shows time shifts of up to 1.5 s between different shot points and occasionally in the same shot gather (Figure 2c). Accordingly, if we assume that P-wave velocities do not vary significantly along the seismic transect, an asymmetry has to be addressed at a Moho level to explain the travel time values and critical distances of PmP. Note that in shot record 3 (Figure 2c), the S branch of the PmP features a relatively high moveout that could be associated to a northward-dipping Moho interface.

Figure 3 shows the raytracing for shots 1 and 3 over the model obtained for the SIMA profile. The length of the profile after projection to a straight line is around 550 km. However, no significant information was obtained to the N, from 450 to 550 km, in the Rif area (Figure 1), probably due to the lack of energy and the lesser resolution implied by an increase in the station spacing. Accordingly, the model there follows the preliminary results of the RIFSIS experiment [*Carbonell et al*., 2013; *Gil et al*., 2013], coincident with the SIMA profile to the N of the Middle Atlas but with shot points distributed all the way up to the northern end.

For the rest of the profile, we have modeled a crust divided in three layers, namely sediments, upper crust, and lower crust (Figures 3 and 4). These layers are constrained by the recognition of the five phases described above; Ps from the sediments, Pg from the boundary between sediments and basement/upper crust, PiP from the upper/lower crust boundary, and PmP and Pn from the crust/mantle boundary. The structure and velocity of the sediments is well constrained by surface data [*Arboleya et al*., 2004; *Teixell et al*., 2003] and Vp apparent values. Maximum sediment thickness is found in the High Atlas and the Middle Atlas (3.7 and 2.6 km, respectively, to the base of the Mesozoic sediments). The Saiss Basin [*Bargach et al*., 2004] is modeled as filled with low Vp sediments (2.6–3.5 km/s, Figure 4) down to a depth of 4.5 km, although the low amplitude of the phases recorded by the stations deployed in the area impedes a precise interpretation. An intracrustal phase (PiP) constrains the existence of a boundary that separates the upper and the lower crust. This phase is not observed in all the records but the travel times and distances it shows in shots 1 and 3 indicate a change in the depth at which this boundary is detected: 17 km from 260 to 380 km, i.e., the segment sampled by shot 1 and 2 (Figures 2a and 2b), and 19 to 27 km from the southern end of the profile to 210 km, the interval sampled for shots 3 and 4 (Figures 2c and 2d). The same structure is observed for the Moho boundary in terms of change of relative depth. While in the area to the N of 270 km the crust/mantle boundary is modeled at ~31 km, to the S, a crustal root places this boundary at a maximum depth of 40–41 km at 240 km, to the N of the High Atlas. From there to the southern end of the profile, the Moho shallows progressively up to depths of 35 km.

Figure 4 shows the velocity model obtained for the SIMA profile. The position of the crustal interfaces is accompanied by a color scale that shows the Vp values for the addressed crustal structure. The geometry of the boundaries is not entirely constrained by raytracing and the areas sampled by incidence rays are marked with a black discontinuous line. Also, the northern part of the profile has no constraints from the SIMA data set. There, the model simply approaches the results of the RIFSIS experiment [*Carbonell et al*., 2013; *Gil et al*., 2013] and does not intend to provide a structure for the Rif Mountains. The High and Middle Atlas mesozoic sediments show Vp that range from 4 to 5 km/s at the surface to 5.3 km/s at the bottom of the sedimentary layer. There are two exceptions to these Vp values, the first one at ~100 km, associated to the very porous cretaceous sediments (Vp = 2.5–3.5 km/s) exposed south of the High Atlas (Figure 1), which absorbed the seismic signal of shot 5 hindering the identification of seismic phases other than Pg or a low amplitude PmP. The second one is the Saiss Basin, with values of 2.6–3.5 km/s down to the floor of the modeled basin.

The upper crustal basement has Vp values that range from 5.4 to 5.8 km/s in the upper part to 6.2 to 6.35 km/s in the contact with the lower part of the crust. In the lower crust, Vp varies between 6.4 and 6.6 km/s

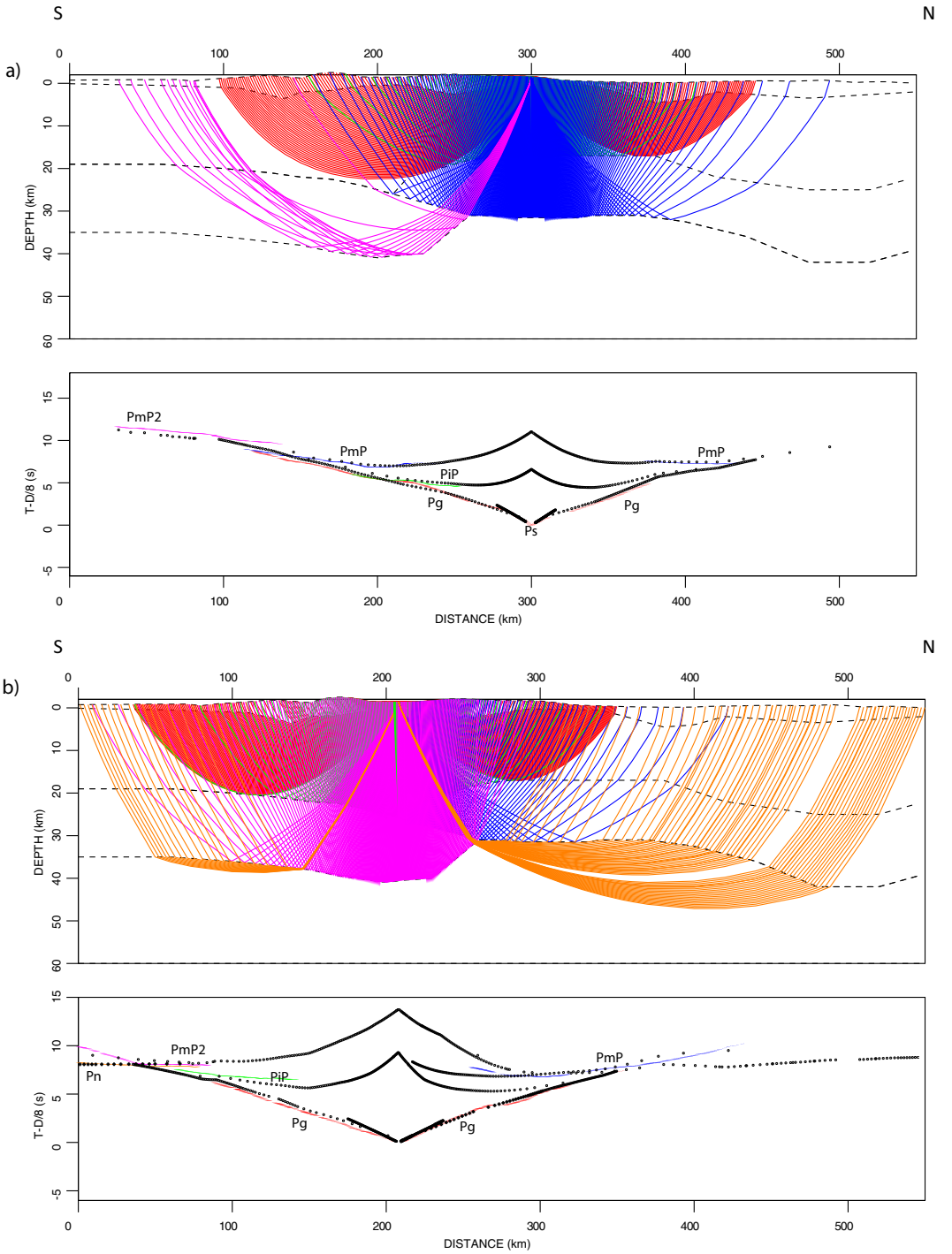

Figure 3. Examples of raytracing over the final velocity model for (a) shots 1 and (b) shots 3 plotted with a Vred = 8 km/s. Color lines are the observed travel time picks and the black lines the modeled ones. Note that for shot 1 (Figure 3a) rays inciding over the Moho give rise to two phases, namely PmP and PmP2, which is observed together with PmP to the S. Shot 3 (Figure 3b) features important differences in the critical distances and travel time of PmP to the N and S that are the key to define a crustal root.

in the upper part to 6.6 and 6.8 km/s at the base. The upper mantle has P-wave velocities that range between 7.6 and 7.8 km/s.

Figure 5 shows the travel time fits between the modeled and the acquired data. The most important deviations appear locally in the upper crust (Pg phase) and also in relation to the crustal root (phases PmP and

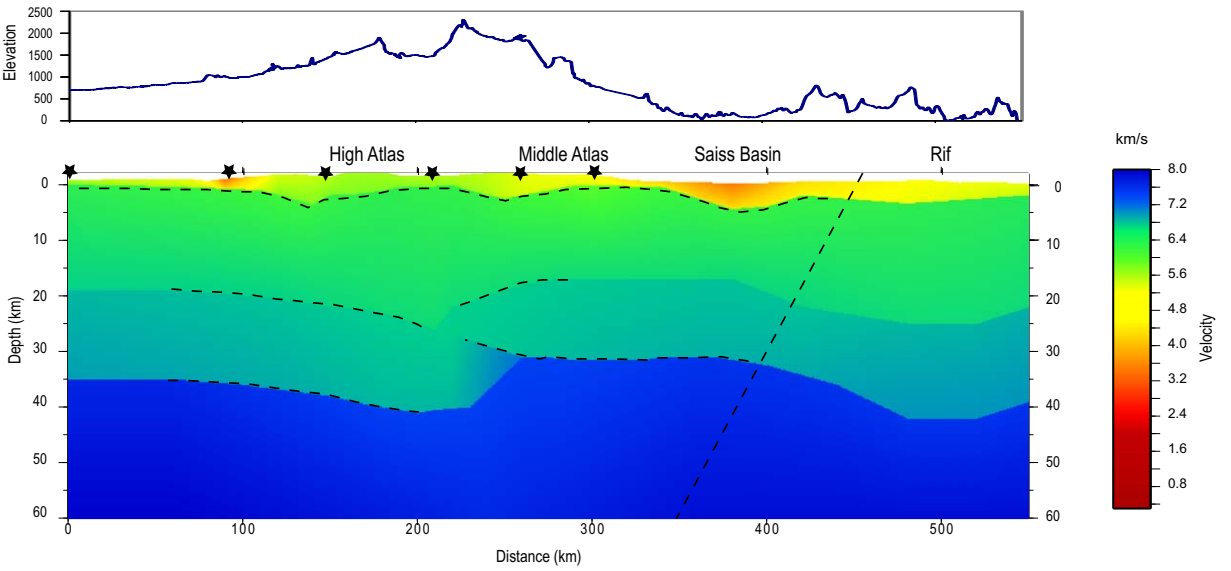

Figure 4. Velocity model obtained after forward modeling (raytracing) of the wide-angle data acquired along the long offset wide-angle reflection SIMA seismic experiment. Dashed lines represent the areas where the boundaries are constrained by incidence rays. Due to the low coverage and lack of resolution, the area to the N of the model (separated with an inclined dash lines, Rif Mountains area) is a sketch of the preliminary results of the RIFSIS experiment and does intend to provide a model for that area (see text).

PmP2). The crooked-line geometry pattern of acquisition, which in some areas precludes to obtain a 2-D image, and the projection of the data to a straight line are the source of these uncertainties. Also, variable topography and local heterogeneities contribute to the existence of local misfits. The altitude at which the stations were deployed has been introduced in the model every 10 km, implying differences between the created topography and the real one of up to ~600 m in the Atlas Mountains. This implies misfits of at least 0.12 s in modeled versus observed travel times, with a maximum that depends on the depth of the interface and of the offset. For 10 km and a shallow interface, where rays travel at higher angles (incidence angle of ~31° for a 3 km deep interface), the difference in travel time could get to 0.2 s for Vp = 5 km/s.

Maximum misfits in the travel times of 0.4 s are found for the PMP2 phase in shot 1. Considering that the elevation of the stations that sample that area has minimum errors (i.e., they lie in a fairly flat area) this error must be mostly caused by the depth or the geometry of the crustal root. Assuming a lower crustal velocity of 6.5 km/s, the observed misfit could be fixed by increasing the depth of the root by about 1.3 km, which would worsen the fit for the Moho arrivals in shots 3 and mostly 4, where this feature gives better PmP phases. In addition, the dip of the Moho is also an issue that should be taken into account. Having in mind that (a) the recording line is most crooked between shots 3 and 4, and that (b) we are imaging a dipping interface with stations that are not perpendicular to it (Figure 1), we acknowledge that we violate the 2-D assumption, giving rise to travel time misfits. Accordingly, the presented model is the one that yields best results for the central shots, where the observed phases are longer, clearer, and provide us with better criteria (i.e., shot 3).

4. Discussion

4.1. Crustal Structure of the Atlas Mountains

Forward modeling carried out over the SIMA wide-angle reflection seismic data indicates that the Atlas crust is imbricated, developing a root slightly N of the High Atlas axis. The location of this crustal root is well constrained by shots 2–4, and especially by shot 3, which shows dramatically different characteristics for the PmP arrivals to the N and S. At the root, the maximum crustal depth reaches ~40–41 km, and it should be underlined that its position does not coincide with that of the highest topography of the High Atlas, but it is displaced to the N. This puzzling feature was already identified after analysis and modeling of gravity data [*Ayarza et al*., 2005]: The trend of the Bouguer anomaly (NE–SW) is oblique to that of the High Atlas (ENE–WSW) thus the High Atlas root has been modeled to the N of the highest topography, coinciding with the minimum Bouguer anomaly values.

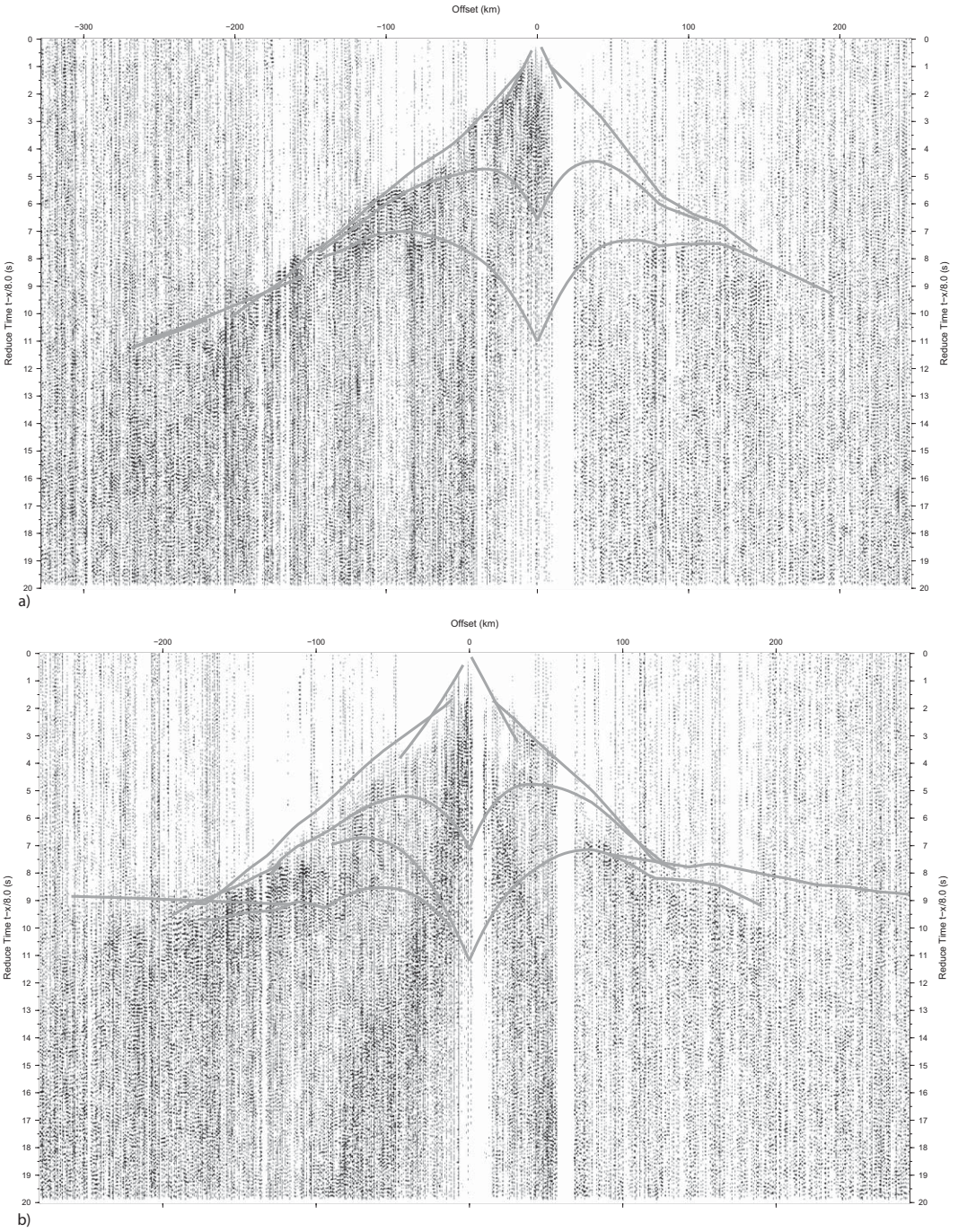

Figure 5. Record sections of shots 1–6 with the theoretical travel-time branches predicted by the P-wave velocity model (Figure 4) overlapped in order to show the fit between observed and modeled data.

The misfit between the location of the Atlas crustal root and that of its highest elevations maybe related with the angle existing between the ENE-WSW regional trend of the High Atlas and that of its internal fault structures (NE-SW), inherited from the mesozoic extension, when the area developed as an oblique rift [*Arboleya et al*., 2004; *El Kochri and Chorowicz*, 1995]. In particular, the root seems to be caused by an orogen-scale, NW-dipping thrust-fault that offsets the Moho and underthrusts the Sahara lower crust to the N (Figures 4 and 6). The structure modeled for the Atlas Mountains is in agreement with that obtained for other inverted continental rifts like the Pyrenees [*Beaumont et al*., 2000; *Choukroune and Team*, 1989;

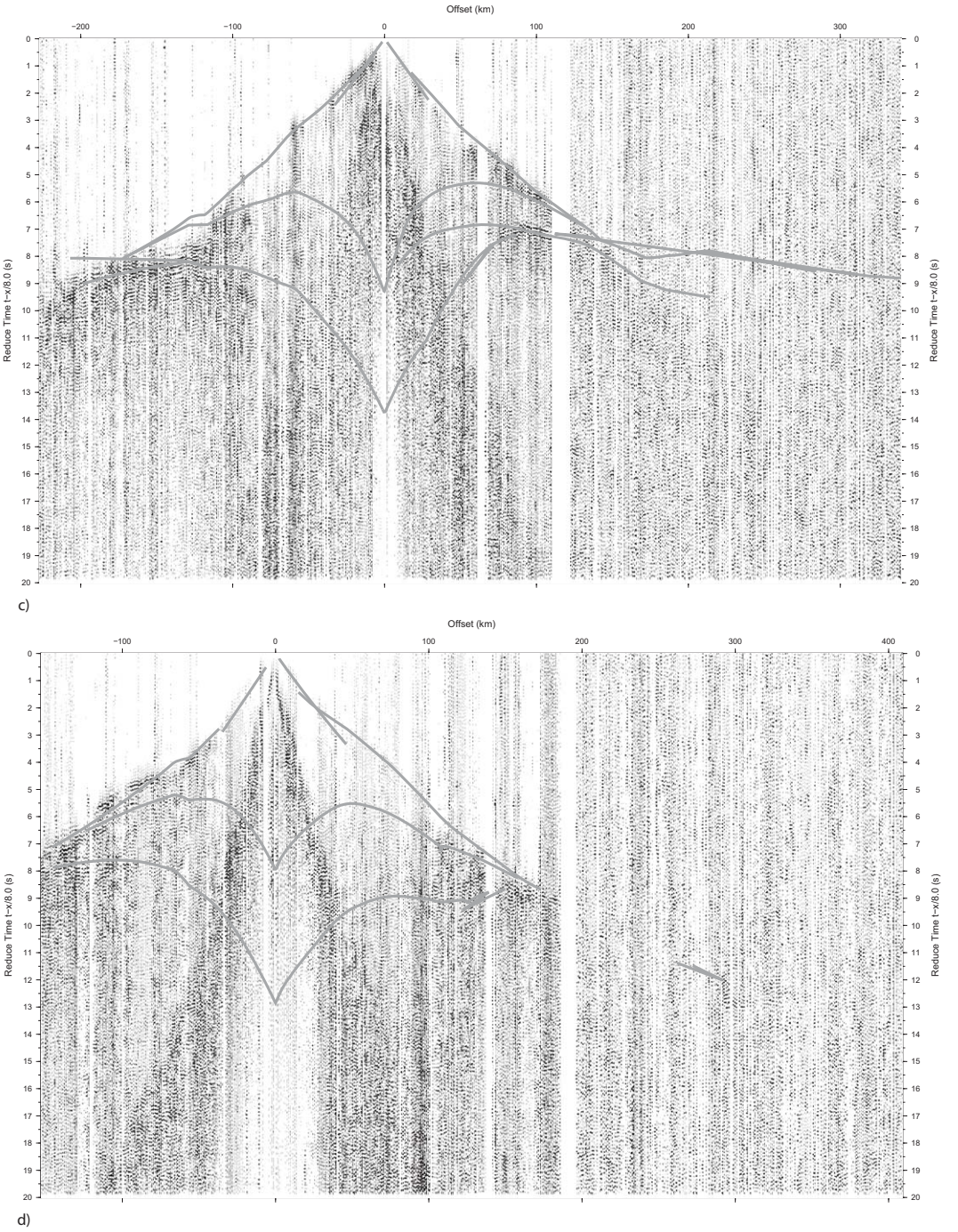

Figure 5. (Continued).

Daignières et al., 1994; *Teixell*, 1998] or the Donbas fold belt [*Maystrenko et al*., 2003], which show thrust offsets of the lower crust and Moho. The model proposed may also explain the two receiver-function velocity jumps (1-D) at 36 and 39 km detected in the Moulouya Plain [*Sandvol et al*., 1998; *Van der Meijde et al*., 2003], which can be regarded as evidence for a Moho duplication. In addition, the crust to the S of the root appears to be thicker than that to the N (>35 km versus ∼31 km). This could respond to the existence of a previous thicker crust to the S and/or to the concentration of deformation and shortening in the southern part of the Atlas. It must be pointed out that forward modeling has not resolved a crustal root under the

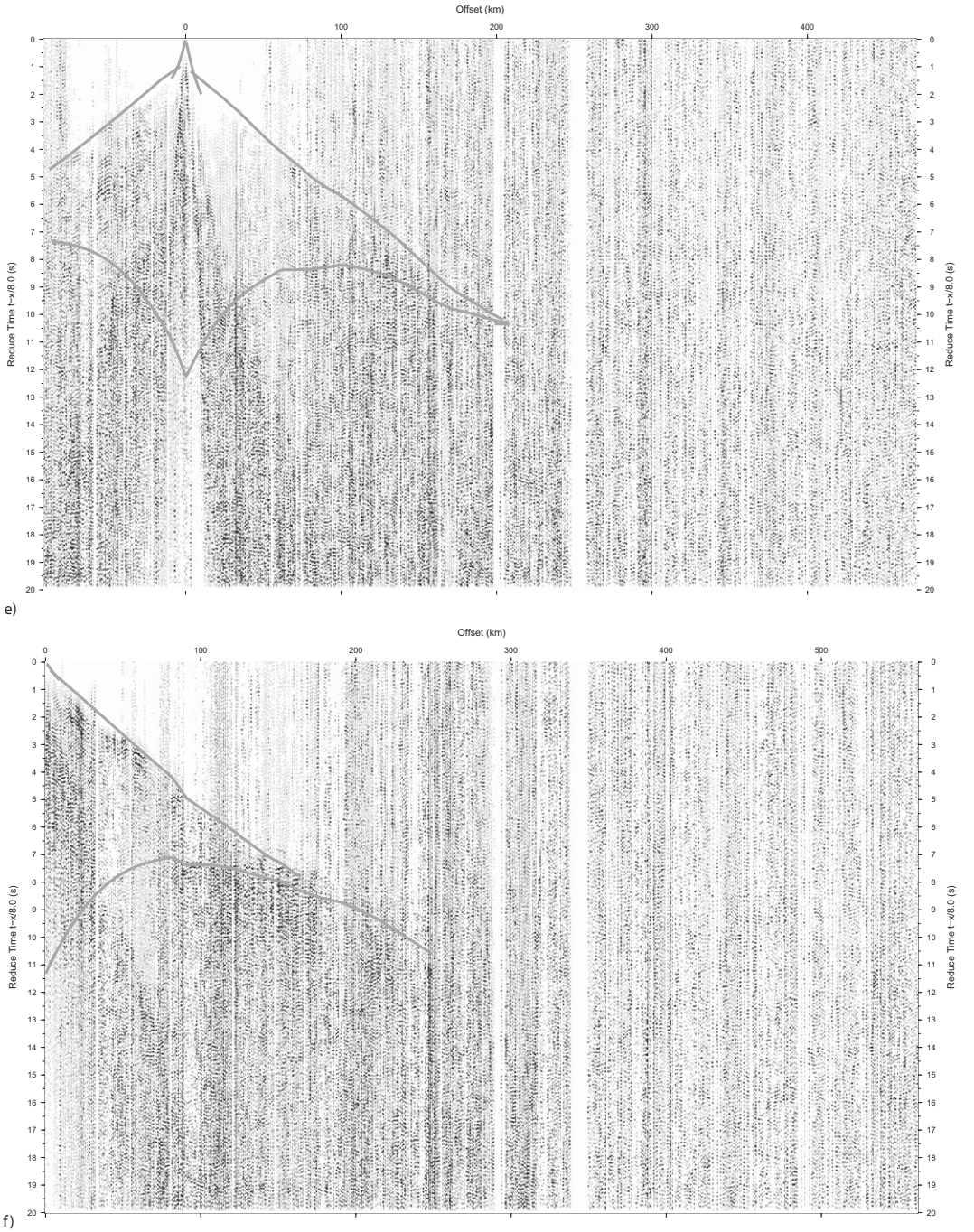

Figure 5. (Continued).

Middle Atlas, which, despite of the high elevations, shows a rather homogeneous crustal thickness (Moho depths of ∼31 km, Figure 4).

Seismicity registered in a 1° band centered along the SIMA recording line is shown in Figure 6 (hypocentres taken from Spanish "Instituto Geográfico Nacional" database). Magnitudes are always below M = 6 and focal depths range between 1 and 185 km, with the deepest earthquakes in the Atlas area. The hypocentres profile shows that seismic activity is high, but most of it is concentrated to the N, in the Rif (and the Alboran Sea) area, near the Africa/Eurasia plate boundary. To the S, seismicity diminishes although some activity is

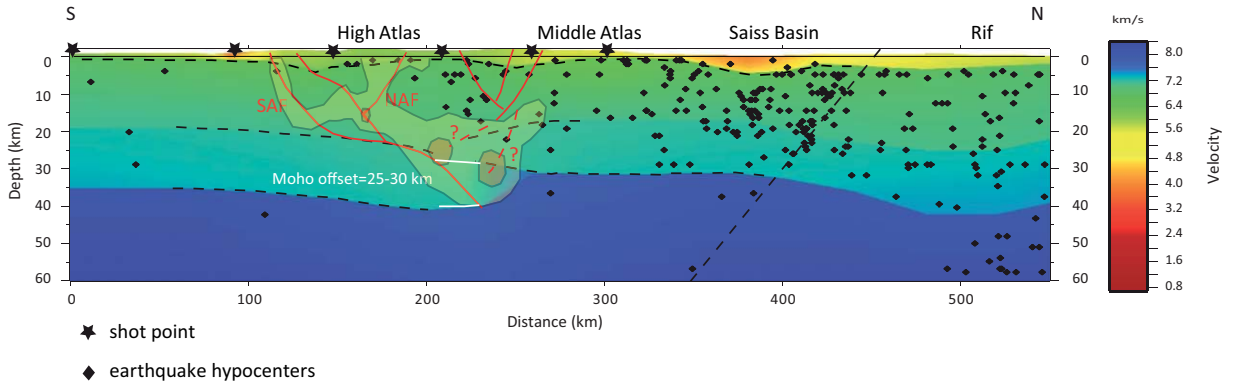

Figure 6. Seismicity across a band of 100 km along the SIMA profile overlain to the velocity model of Figure 4 (data from the Instituto Geográfico Nacional). The tectonic interpretation of this velocity model is also included. The suggested fault pattern in the High Atlas would resolve at depth the shortening estimated through balanced geological sections. White lines indicate the Moho interval that appears overlapped between the Saharan crust and the Atlas crust, and thus, document a Moho thrust offset. Contours and semitransparent colors represent the resistivity model by *Ledo et al.* [2011]: outer contour: yellow; $\rho < 25$ ohm m, inner contour: orange; $\rho < 2$ ohm m. Note the good coincidence between the lower resistivities and the areas of lower velocities, and the position of the mantle wedge proposed to account for an admissible shortening magnitude in the deep crust (see text for explanation). SAF: South Atlas Fault. NAF: North Atlas Fault. Horizontal scale is twice the vertical scale.

recorded along the Middle and High Atlas and the Anti-Atlas. Seismicity also decreases toward the Sahara and to the E of the Atlas Mountains. However, in its western part, earthquake activity has provided information to map two of the most active faults in the area, namely the South Atlas Fault and the North Atlas Fault (Figures 1 and 6) [*Sébrier et al.*, 2006]. Even though the studied seismicity does not allow the authors the calculation of focal depths or mechanisms, the surface trace of these faults coincide with the projection of the epicenters at the surface. The South Atlas Fault might be a conductive feature [*Schwarz et al.*, 1992] and still evidences ongoing tectonic activity [*Pastor et al.*, 2012]. It appears to have accommodated most of the cenozoic shortening of this mountain belt [*Sébrier et al.*, 2006] and accordingly, it may be the key feature that defines the root modeled in this work. On the other hand, most of the seismicity observed along the SIMA transect appears in the upper crust, suggesting that the modeled upper-lower crust transition might represent the brittle/ductile transition, where thrusts that do not cut the entire crust may root.

One important issue under consideration is the length of the underthrust crust. The model here presented, features a duplication of the Atlas lower crust with a length of about 50 km (Figures 4 and 6). However, shortening estimates from balanced cross sections of the High Atlas upper crust reached maximum values of about 25 km [*Teixell et al.*, 2003]. Figure 4 shows that, the structure modeled, is not always constrained by incidence rays and although the boundaries that reflected off the seismic waves strongly point out to the structure depicted, this model may have small deviations from the real structure. On the other hand, the highest travel time misfits appear in the northern part of the root and suggest the existence of higher velocities in this area. In fact, the northern part of the underthrusting crust has slightly higher velocities than the rest of the lower crust, defining a positive lateral Vp gradient (Figures 4 and 6). This feature might represent a change in the physical properties of the N-dipping Saharan crust or an, as yet, undefined mantle wedge. Such a feature could increase the average velocities just enough to fit local travel times, and would decrease the length of the crustal duplication. An interpretation based on this concept is presented in Figure 6. The north dipping South Atlas Frontal Thrust cuts the entire crust running along the upper-lower crust boundary along ~50 km and offsetting the Moho. This deformation pattern implies a Moho offset (i.e., lower crust imbrication) of ~25–30 km, more in agreement with the total shortening estimated from surface data. However, it is important to keep in mind that, stations located between the High and the Middle Atlas do not lie perpendicular to the structures (Figure 1), and thus are not perpendicular to the trend of the inferred crustal root. Such a complicated feature, which locally is not imaged in 2-D, is difficult to address by raytracing. Vp abrupt changes and inversions give rise to complicated ray trajectories, and inverse modeling strategies should be used to better define that area.

The velocity model does not allow us to make interpretations about how the shortening might be accommodated at depth in the Middle Atlas. Accordingly, the deep faults traced in Figure 6 represent just alternative possibilities: faults rooting in the upper-lower crust boundary, in the Moho, or even with a small offset of the latter.

4.2. Significance of P-Wave Velocity Distribution Along the SIMA Transect

The main characteristic of the Atlas crust and upper mantle are the low P-wave velocities found for the entire modeled transect, but most importantly, for the Middle and High Atlas segment. Vp values of 6.4–6.6 km/s characterize the top and bottom of the lower crust in the root area and in the Middle Atlas. The uppermost mantle shows also low Vp values, always below 7.8 km/s. Even though we only observed Pn phases in 4 shots, and that in some instances, they appear along short offsets, their apparent velocity is always below 8 km/s, even in the case of up-dip phases (Figure 2b).

The Atlas Mountains host a relatively high geothermal gradient, and high heat flow values of up to 100 mWm^{-2} have been measured [*Rimi*, 1999]. These values do not necessarily imply the existence of a hot crust and mantle, but the low Vp velocities found with the SIMA data set reinforce this idea. Low seismic velocities have been often related to high temperatures and to the existence of partial melts [*Dunn and Forsyth*, 2003; *Hammond and Humphreys*, 2000]. In fact, melting has a quantitative effect on seismic wave velocity, mostly in S waves, but also in P-waves, since it implies a contrast in the elastic properties of materials (poroelastic effect) and an enhanced wave attenuation and dispersion (anelastic effect) [*Karato and Spetzler*, 1990]. However, the small amounts of melt present in areas with important Vs decrease, bring to the debate whether it is the melts or just the increase of temperature that reduces the seismic wave velocities. Even though grain size is still an issue, laboratory experiments indicate that Vs is more strongly affected by the increase in temperature than by the presence of melt itself [*Priestley and McKenzie*, 2006].

The Atlas Mountains present evidences of volcanic activity from the Eocene to present, with a maximum in the past 15 Ma. In the area between the north High Atlas front and the Middle Atlas, three episodes of alkaline volcanism have been recognized, the last of them Quaternary in age [*Harmand and Cantagrel*, 1984], and have been interpreted as asthenospheric in origin [*El Azzouzi et al*., 1999].

On the other hand, recent long-period MT experiments revealed the existence of a conductive anomaly (resistivity, $\rho < 8\ \Omega$ m) in the High Atlas upper mantle. This feature seems to connect with the surface in the quaternary volcanic province of the Middle Atlas, and is interpreted as an anomalously shallow melted mantle [*Anahnah et al*., 2011]. Even in the lower crust underneath the Moulouya Plain (Figure 1), a low-resistivity anomaly ($\rho < 4$ ohm m), which coincides well the crustal structure here presented (Figure 6), is related to the lack of seismicity in this area and explained by the existence of 2–8% of partial melt [*Ledo et al*., 2011]. In this regard, studies of lower crust xenoliths from the Middle Atlas lavas are in progress. The first observations suggest that there are partial melts similar to those found in the metapelitic xenolith suites from the Neogene Volcanic Province of SE Spain (Alvarez-Valero, personal communication, 2013), which were originated by partial melting at different crustal depths. In that area, the depth at which partial melt has been identified coincides with a low velocity zone inferred by seismic studies [*Alvarez-Valero and Kriegsman*, 2007].

Taking into account these considerations, we suggest that the very low P-wave velocity values found in the lower crust and mantle of the Middle and High Atlas are caused by high temperatures and partial melt at those levels. This idea is supported by the young volcanism in the Middle Atlas and is in agreement with the models obtained for neighboring areas [*Alvarez-Valero and Kriegsman*, 2007]. The occurrence of low Vp values in the Atlas Mountains was also addressed by *Tadili et al*. [1986] and *Wigger et al*. [1992]. Although the resulting velocity models are different, the later authors include, in the lower crust and mantle under the northern High Atlas, very low velocity layers of 6 and 6.3 km/s that would contribute to average velocity values down to those found in our model. On the other hand, the high reflectivity and the complex pattern observed for lower crust and mantle phases to the S of the shot point 2 (Figure 2b) indicate high velocity contrasts that may respond to areas of partial melt or to underplating phenomena linked to the volcanic activity of the Middle Atlas. Similar features have been found in the Basin and Range Province [*Benz et al*., 1990], where high heat flow values (90 mW/m^2), Cenozoic magmatism and low (but high gradient) Vp velocities in the lower crust (6.4 to 6.6–6.8 km/s) have been related to high pore pressure and to a compositional change with depth geared by magmatic intrusions and underplating. Furthermore, resistivity in the Atlas lower crust and mantle is lower than that in the Basin and Range (0–8 ohm m versus 30–100 ohm m) and accordingly, higher pore pressure is expected. The models that relate conductivity and porosity

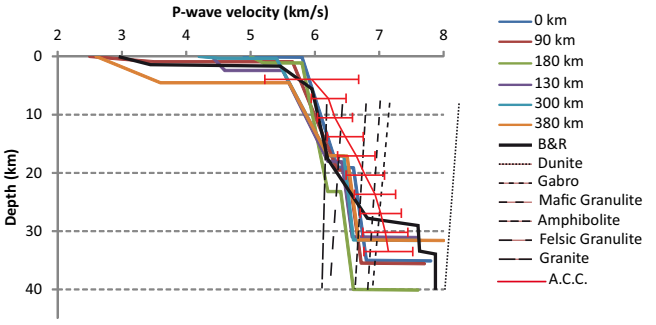

Figure 7. Vp profiles over six localities along the SIMA profile (color lines). Black bold line represents the Vp-depth profile over one characteristic location at the Basin and Range (B&R) as presented in *Benz et al*. [1990]. Discontinuous lines represent the Vp-depth profiles calculated by *Benz et al*. [1990] for a continental crust and mantle, using heat flow values of 90 mWm^{-2} and an average crustal density of 2.8 kg/m^3. Red continuous line represents the average continental crust (ACC) P-wave velocities [*Christensen and Mooney*, 1995]. The average Vp obtained for the Atlas lower crust and mantle are lower than those found in ACC and similar to the ones found in the B&R. Gradients are higher in the upper crust and less important in the lower crust, although still reaching values that may indicate lithological changes with depth (compare with gradients derived for constant compositions).

[*Hyndman and Klemperer*, 1989] indicate that resistivities, $\rho < 10$ ohm m may account for a Vp decrease of 8%, i.e., from 7 to 6.44 km/s.

Recent Rayleigh wave tomography data [*Palomeras et al*., 2013] show that the S-wave velocity structure of the Atlas Mountains contrasts with that of the surrounding areas in Morocco. In their models, these authors show that the shear wave velocity structure varies with depth and matches that found for P-waves and presented in this paper. Even though the data set used by *Palomeras et al*. [2013] has lesser resolution than the SIMA data set, there is good agreement in both models at a depth of 35 km, where shear waves show a decrease of about 5% in the northern part of the High Atlas. This Vs decrease may correspond to our modeled crustal root, which places the base of the lower crust at depths below 35 km (Figure 4) causing the Vp to decrease in relation to the surrounding mantle.

4.3. Constraints on the (Lower) Crust Composition

The SIMA data set indicates that the Atlas crust is divided in three layers, out of which only one of them never crops out: the lower crust. In order to make some assessment about the lower crustal composition, indirect methods should be recalled, one of them being the study of seismic wave velocity. P-wave velocities keep a relationship with the density and elastic constants of the materials, and therefore, vary depending on the rock type. However, it is difficult to address crustal compositions from Vp values alone in highly conductive environments [*Hyndman and Klemperer*, 1989] that might have high pore pressure and the existence of partial melt.

Given the observed heat flow values in the Atlas Mountains, high temperatures can be assumed to exist at lower crust levels, and thus, a granulite grade metamorphism may be expected. In fact, lower crustal granulitic xenolithes have already been identified in the Middle Atlas lavas and are under study (Alvarez Valero, personal communication). However, the Vp values found at those levels are lower than those expected for the granulite rock type. At increasing temperatures, the Vp of granulites decreases importantly, up to an 8% decrease from 0 to ~500°C at 2 Kb [*Christensen*, 1979], and this may account for Vp inversions. If the effect of pressure is added, Vp remains close to constant with depth [*Benz et al*., 1990] and Vp gradients must be explained by lithological changes.

Figure 7 shows six 1-D, Vp-depth profiles extracted from the model at 0, 90, 180, 260, 300, and 360 km of distance. These locations have been chosen because they are representative of different tectonic zones. Also in Figure 7, we present the (a) Vp-depth profile derived for one representative location of the Basin and Range (SP1) [*Benz et al*., 1990], (b) Vp-depth profile for an average continental crust (ACC) [*Christensen and Mooney*, 1995], and (c) the Vp-depth profiles calculated for continental crust and mantle rocks with an average density of 2.8 kg/m^3 and a heat flow of 90 mWm^{-2} [*Benz et al*., 1990]. Although the later profiles were calculated to compare with the Basin and Range Vp structure, the parameters used (see above) match those expected and measured in the Atlas Mountains.

In general, the Atlas velocity profile present lower values than the ACC and similar to those of the Basin and Range. The only difference lies in the depth at which crustal P-wave velocities switch to mantle velocities and are attributable to the different crustal thickness of both areas. The Vp profiles calculated from the data used in this paper show a constant increase of Vp with depth, first with a high gradient and then with a smoother gradient below the upper/lower crust boundary. In general, a positive Vp gradient is related to a

decrease in the porosity as depth increases and/or to lithological changes. The first assumption may apply to the sediments and upper crust. However, the lower crust of the Atlas Mountains shows low P-wave velocities with a gentle positive gradient, smoother than that observed for the Basin and Range, but stronger than that expected for single-lithology deep crustal rocks. Granulite's Vp velocities (Figure 7) are around 7 km/s for mafic granulites and close to 6.4–6.5 km/s for felsic granulites. Those velocities remain fairly constant or show negative gradients in a range from 10 to 30 km depth, suggesting that gradients found in the SIMA data may depend on lithological changes. An alternation of felsic and mafic granulites in the lower crust could account for the average velocities we observe in this level. The gradient, however, must be explained by an increase in mafic components with depth, probably related with continuous intrusion processes affecting the crust since the Mesozoic, first in relation to Triassic-Jurassic rifting, later to the Tertiary to recent asthenospheric upwelling and volcanism. We have seen that underplating processes may be invoked to explain high reflectivity at the base of the crust of the Middle Atlas. Partial melt probably existing at deep crustal levels make the Atlas Vp gradients values slightly lower than those of the Basin and Range.

4.4. Implications of the Results on the Atlas Lithospheric Model

Potential field-based lithospheric models attempted to explain the inconsistency between topography and shortening in the Atlas Mountains, assuming that isostatic balance exist at a LAB level. Those models argue that, depending on crustal thickness, a mantle upwelling might bring the asthenosphere as high as $\sim$70 km in order to support the mountain building [*Teixell et al*., 2005; *Zeyen et al*., 2005]. The crustal thickness used to map the LAB was deduced from previous low-resolution seismic refraction [*Tadili et al*., 1986; *Wigger et al*., 1992] and gravity data [*Ayarza et al*., 2005]. These data sets place the Moho at a maximum of 39–40 km depth in the root and between 35 and 37 km elsewhere in the Atlas area.

The results obtained in the present work imply slight modifications to the previous models. We still suggest that, along the section sampled by the SIMA profile, the Atlas Mountains have a modest crustal root that gets to $\sim$40–41 km depth and accounts for its low gravity Bouguer anomaly. However, we have found significant differences in the crustal thickness to the N and S of that root, allowing us to distinguish a Middle Atlas crust, with an average thickness close to 32 km (depth to the Moho $\sim$31 km), and a thicker High Atlas crust, of $>$35 km in the southern end of the profile. These values will slightly modify the position of the LAB if isostatic equilibrium is assumed, and even though it will not change much its uppermost part, it might introduce variations in its geometry, making it a bit shallower to the S but especially to the N of the root area, in the Middle Atlas. In fact, shear wave tomography based on Rayleigh teleseismic waves places the base of the lithosphere at 50 km underneath the Atlas [*Palomeras et al*., 2013], which would be in agreement with a thinner crust and thus would imply a more important contribution of the asthenosphere in the Atlas topography.

In view of all the new data acquired recently, multidisciplinary interpretations in which all data sets are integrated must be carried out in order to precisely locate the most important lithospheric interfaces in the Atlas Mountains and to approach to a better constrained model of the Atlas orogen.

5. Conclusions

A 700 km long, high-resolution, controlled source, wide-angle seismic reflection profile has been acquired across the Moroccan Atlas and Rif Mountains in spring 2010 (SIMA profile). Its main goals were to unravel the mechanisms that support the Atlas topography by improving the knowledge of the position and geometry of crustal interfaces, including the Moho, and by helping to constrain the depth of an anomalously shallow modeled LAB boundary.

The SIMA data set has an irregular signal/noise ratio, with almost no signal to the N, in the Rif area, relatively good resolution in the Atlas area, and low amplitude signal in the southernmost part of the profile, in the Saharan craton. Forward modeling of P-waves constrains a section of 300 km centered in the High and Middle Atlas and outlines a model with a three-layers crust, representing the Mesozoic and Tertiary sediments (Vp = 2–5.5 km/s), the basement/upper crust (Vp = 5.8–6.35 km/s) and the lower crust (Vp = 6.4–6.8 km/s). The Atlas mantle shows low Vp values that never exceed 7.8 km/s. A midcrustal discontinuity is placed between 17 and 24 km depth and implies a smooth velocity increase of 0.1–0.15 km/s. This interface might act as a local detachment between upper and lower crust and represents the boundary where some upper

crustal thrusts sole out. However, a N to NW-dipping main thrust cuts the entire crust and Moho discontinuity, producing a crustal root in the northern part of the High Atlas. Its location agrees fairly well with that of the minimum Bouguer gravity anomaly values and its depth reaches 40–41 km below sea level. To the N and S of the root the crust is thinner, getting to depths of 31 km and 35–38 km, respectively, suggesting different deformation history and/or contrasting predeformation thicknesses of both crusts. The modeled structure suggests that shortening involves the deep crust although, in the present model, the duplicated lower crust would amount higher shortening than that estimated from balanced sections of the High Atlas upper crust. Alternative features as an overthrusting mantle wedge in the root zone can be preliminary suggested in order to compensate the shortening estimated at the surface. On the other hand, forward modeling failed to detect a crustal root under the Middle Atlas.

The low Vp values obtained in the lower crust and mantle of the Middle and High Atlas are thought to represent the existence of high temperatures and partial melts at these levels. These results are in agreement with the elevated heat flow and conductivities reported for the same area, and are probably a consequence of the Tertiary-to-present magmatic activity of the Atlas region. In this regard, high reflectivity observed in the Middle Atlas deep crust is interpreted as due to magmatic intrusions and underplating.

Potential field lithospheric models of the Atlas Mountains should be revisited to allow the inclusion of new data sets acquired in recent years. Lower P-wave velocities might indicate slightly lower densities that could modify the existing gravity models. The Moho geometry modeled in this work also implies changes in the pattern of the lithosphere/asthenosphere boundary. However, the present data set further favors the need of a mantle contribution to support the high topography the Atlas Mountains.

Acknowledgments

This work has been primarily funded by the Spanish MEC project CGL2007–63889. Additional funding was provided by projects CGL2010–15416, CSD2006-00041, and CGL2009–09727 (Spain), CGL2008–03474-E, 07-TOPO_EUROPE_FP-006 (ESF Eurocores) and EAR-0808939 (US, NSF). Seismic stations were kindly provided by IRIS-Passcal. We thank the numerous geoscientists from Spanish, Moroccan, and US institutions that helped with the station deployment along the profile trace. The IS Rabat facilitated access to the Ifrane Geophysical Station which was the operation center during the seismic acquisition. This manuscript benefitted from helpful comments received from two anonymous reviewers. The data used in this research are available upon request to R. Carbonell.

References

Alvarez-Valero, A. M., and L. M. Kriegsman (2007), Crustal thinning and mafic underplating beneath the Neogene Volcanic Province (Betic Cordillera, SE Spain): Evidence from crustal xenoliths, *Terra Nova 19*, 266–281.

Anahnah, F., et al. (2011), Deep resistivity cross section of the intraplate Atlas Mountains (NW Africa): New evidence of anomalous mantle and related Quaternary volcanism, *Tectonics*, *30*, 1–9.

Anguita, F., and F. Hernan (2000), The Canary Islands origin: A unifying model, *J. Volcanol. Geotherm. Res.*, *103*(1–4), 1–26.

Arboleya, M. L., A. Teixell, M. Charroud, and M. Julivert (2004), A structural transect through the High and Middle Atlas of Morocco, *J. Afr. Earth Sci.*, *39*, 319–336.

Ayarza, P., F. Alvarez-Lobato, A. Teixell, M. L. Arboleya, E. Teson, M. Julivert, and M. Charroud (2005), Crustal structure under the central High Atlas Mountains (Morocco) from geological and gravity data, *Tectonophysics*, *400*, 67–84.

Bargach, K., P. Ruano, A. Chabli, J. Galindo-Zaldivar, A. Chalouan, A. Jabaloy, M. Akil, M. Ahmamou, C. Sanz de Galdeano, and M. Benmakhlouf (2004), Recent tectonic deformations and stresses in the frontal part of the Rif Cordillera and the Saïss Basin (Fes and Rabat Regions, Morocco), *Pure Appl. Geophys.*, *161*, 521–540.

Beauchamp, W., R. W. Allmendinger, M. Baranzagi, A. Demnati, M. El Alji, and M. Dahmani (1999), Inversion tectonics and the evolution of the High Atlas Mountains, Morocco, based on a geological/geophysical transect, *Tectonics*, *18*, 163–185.

Beaumont, C., J. A. Muñoz, J. Hamilton, and P. Fullsack (2000), Factors controlling the Alpine evolution of the central Pyrenees inferred from a comparison of observations and geodynamical models, *J. Geophys. Res.*, *105*, 8125–8145.

Benz, H. M., R. B. Smith, and W. D. Mooney (1990), Crustal structure of the northwestern Basin and Range Province from the 1986 program for array seismic studies of the Continental Lithosphere Seismic Experiment, *J. Geophys. Res.*, *95*, 21,823–21,842.

Bijwaard, H., and W. Spakman (2000), Non-linear global P-wave tomography by iterated linear inversion, *Geophys. J. Int.*, *141*, 71–80.

Carbonell, R., A. Pérez Estaún, J. Gallart, J. Díaz, S. Kashubin, J. Mechie, R. Stadtlander, A. Schulze, J. H. Knapp, and A. Morozov (1996), Crustal root beneath the Urals: Wide-angle seismic evidence, *Science*, *274*, 222–224.

Carbonell, R., J. Gallart, A. Pérez-Estaún, J. Diaz, S. Kashubin, J. Mechie, F. Wenzel, and J. Knapp (2000), Seismic wide-angle constraints on the crust of the southern Urals, *J. Geophys. Res.*, *105*, 13,755–13,777.

Carbonell, R., et al. (2013), A 700 km long crustal transect across northern Morocco, *Geophys. Res. Abstr.*, *EGU2013-8313*, 15.

Choukroune, P., and E. Team (1989), The ECORS Pyrenean deep seismic profile reflection data and the overall structure of an orogenic belt, *Tectonics*, *8*, 23–39.

Christensen, N. I. (1979), Compressional wave velocities in rocks at high temperatures and pressures, critical thermal gradients, and crustal low-velocity zones, *J. Geophys. Res.*, *84*, 6849–6857.

Christensen, N. I., and W. D. Mooney (1995), Seismic velocity structure and composition of the continental crust: A global view, *J. Geophys. Res.*, *100*, 9761–9788.

Daignières, M., M. Séguret, M. Specht, and E. Team (1994), The Arzacq-Western Pyrenees ECORS Deep Seismic Profile, *Eur. Assoc. Petrol. Geol. Spec. Publ.*, *4*, 199–208.

Dunn, R. A., and D. W. Forsyth (2003), Imaging the transition between the region of melt generation and crustal magma chamber beneath the southern East Pacific Rise with short-period Love waves, *J. Geophys. Res.*, *108*(B7), 2352, doi:10.1029/2002JB002217.

El Azzouzi, M., J. Bernard-Griffiths, H. Bellon, R. C. Maury, A. Piqué, S. Fourcade, J. Cotten, and J. Hernandez (1999), Evolution des sources du volcanisme marocain au cours du Néogène, *Compt. Rendus de l'Acad. des Sci. Paris*, *329*, 95–102.

El Kochri, A., and J. Chorowicz (1995), Oblique extension in the Jurassic trough of the central and eastern High Atlas (Morocco), *Can. J. Earth Sci.*, *33*, 84–92.

Flecha, I., I. Palomeras, R. Carbonell, F. Simancas, P. Ayarza, J. Matas, F. González-Lodeiro, and A. Pérez-Estaún (2009), Seismic imaging and modelling of the lithosphere of SW-Iberia, *Tectonophysics*, *472*, 148–157.

Frizon de Lamotte, D., B. Saint Bezar, R. Bracène, and E. Mercier (2000), The two main steps of the Atlas building and geodynamics of the western Mediterranean, *Tectonics*, *19*, 740–761.
Frizon de Lamotte, D., M. Zizi, Y. Missenard, M. Hafid, M. El Azzouzi, R. C. Maury, A. Charrière, Z. Taki, M. Benammi, and A. Michard (2008), The Atlas system, in *Continental Evolution: The Geology of Morocco*, edited by A. Michard, pp. 133–202, Springer-Verlag, Berlin.
Fullea, J., M. Fernandez, J. C. Afonso, J. Verges, and H. Zeyen (2010), The structure and evolution of the lithosphere-asthenosphere boundary beneath the Atlantic-Mediterranean transition region, *Lithos*, *120*, 74–99.
Giese, P., and V. Jacobshagen (1992), Inversion tectonics of intracontinental ranges: High and middle Atlas, Morocco, *Geol. Rundsch.*, *81*, 249–259.
Gil, A., J. Gallart, J. Díaz, R. Carbonell, M. Harnafi, and A. Levander (2013), Crust structure across the Rif Cordillera from 'RIFSIS' seismic refraction and wide-angle reflection experiment, *Geophys. Res. Abstr.*, *EGU2013-4887-1*, 15.
Gómez, F., W. Beauchamp, and M. Barazangi (2000), Role of Atlas Mountains (northwest Africa) within the African/Eurasian plate boundary zone, *Geology*, *28*, 775–778.
Hammond, W. C., and E. D. Humphreys (2000), Upper mantle seismic wave velocity: Effects of realistic partial melt geometries, *J. Geophys. Res.*, *105*, 10,975–10,986.
Harmand, C., and J. M. Cantagrel (1984), Le volcanisme alcalin Tertiaire et Quaternaire du Moyen Atlas (Maroc): Chronologie K/Ar et cadre géodynamique, *J. Afr. Earth Sci.*, *2*, 51–55.
Hoernle, K., Y. Zhang, and D. Graham (1995), Seismic and geochemical evidence for large-scale mantle upwelling beneath the eastern Atlantic and western and central Europe, *Nature*, *334*, 334–339.
Hyndman, R. D., and S. L. Klemperer (1989), Lower-crustal porosity from electrical measurements and inferences about composition from seismic velocities, *Geophys. Res. Lett.*, *16*, 255–258.
Karato, S., and H. A. Spetzler (1990), Defect microdynamics in minerals and solid-state mechanisms of seismic wave attenuation and velocity dispersion in the mantle, *Rev. Geophys.*, *28*, 399–421.
Laville, E., and A. Piqué (1992), Jurassic penetrative deformation and Cenozoic uplift in the central High Atlas (Morocco): A tectonic model, structural and orogenic inversions, *Geol. Rundsch.*, *81*, 157–170.
Laville, E., J.-L. Lesage, and M. Seguret (1977), Géométrie, cinématique (dynamique) de la tectonique atlasique sur le versant sud du Haut Atlas marocain. Aperçu sur les tectoniques hercyniennes et tardihercyniennes, *Bull. Soc. Géol. France*, *7*, 527–539.
Ledo, J. J., A. G. Jones, A. Siniscalchi, J. Campanyàa, D. Kiyan, G. Romanoc, M. Rouaid, and T. M. Team (2011), Electrical signature of modern and ancient tectonic processes in the crust of the Atlas mountains of Morocco, *Phys. Earth Planet. Inter.*, *185*, 82–90.
Mattauer, M., P. Tapponier, and F. Proust (1977), Sur les mécanismes de formation des chaines intracontinentales. L'exemple des chaines atlasiques du Maroc, *Bull. Soc. Géol. Fr.*, *7*, 521–536.
Maystrenko, Y., et al. (2003), Crustal-scale pop-up structure in cratonic lithosphere: DOBRE deep seismic reflection study of the Donbas fold belt, Ukraine, *Geology*, *31*, 733–736.
Medina, F., and T. Cherkaoui (1991), Focal mechanisms of the Atlas earthquakes and tectonic implication, *Geol. Rundsch.*, *3*, 639–650.
Morel, J.-L., M. Zouine, and A. Poisson (1993), Relations entre la subsidence des bassins moulouyens et la création des reliefs atlasiques (Maroc): Un exemple d'inversion tectonique depuis le Néogene, *Bull. Soc. Géol. Fr.*, *93*, 79–91.
Morel, J.-L., M. Zouine, J. Andrieux, and A. Faure-Muret (2000), Déformations néogeènes et quaternaires de la bordure nord haut atlasique (Maroc): Rôle du socle et conséquences structurelles, *J. Afr. Earth Sci.*, *30*, 119–131.
Palomeras, I., R. Carbonell, I. Flecha, F. Simancas, P. Ayarza, J. Matas, D. M. Poyatos, A. Azor, F. G. Lodeiro, and A. Pérez-Estaun (2009), Nature of the lithosphere across the Variscan orogen of SW Iberia: Dense wide-angle seismic reflection data, *J. Geophys. Res.*, *114*, B02302, doi: 10.1029/2007JB005050.
Palomeras, I., R. Carbonell, P. Ayarza, D. Martí, D. Brown, and J. F. Simancas (2011), Shear wave modeling and Poisson's ratio in the Variscan Belt of SW Iberia, *Geochem. Geophys. Geosyst.*, *12*, Q07008, doi:10.1029/2011GC003577.
Palomeras, I., S. Thurner, A. Levander, K. Liu, A. Villaseñor, and R. Carbonell (2013), Finite-frequency Rayleigh wave tomography of the Western Mediterranean, *Geochem. Geophys. Geosyst.*, *15*, 140–160, doi:10.1002/2013GC004861.
Pastor, A., A. Teixell, and M. L. Arboleya (2012), Rates of Quaternary deformation in the Ouarzazate basin (Southern Atlas Front, Morocco), *Ann. Geophys.*, *55*, 1003–1016.
Priestley, K., and D. McKenzie (2006), The thermal structure of the lithosphere from shear wave velocities, *Earth Planet. Sci. Lett.*, *244*, 285–301.
Prodehl, C., and W. D. Mooney (2012), Exploring the earth's crust-history and results of controlled source seismology, *Mem. Geol. Soc. Am.*, *208*, 1–779.
Ramdani, F. (1998), Geodynamic implications of intermediate-depth earthquakes and volcanism in the intraplate Atlas Mountains (Morocco), *Phys. Earth Planet. Inter.*, *108*, 245–260.
Rimi, A. (1999), Mantle heat flow and geotherms for the main geologic domains in Morocco, *Int. J. Earth Sci.*, *99*, 458–466.
Sandvol, E., A. Calvert, and M. Barazangui (1998), Grid search modelling of receiver functions: Implications for crustal structure in the Middle East and North Africa, *J. Geophys. Res.*, *103*(B11), 26,899–26,917.
Schwarz, G., H. G. Mehi, H.G. Ramdani, and V. Rath (1992), Electrical resistivity structure of the eastern Moroccan Atlas System and its tectonics implications, *Geol. Rundsch.*, *81*, 221–235.
Seber, D., M. Barazangi, B. Tadili, M. Ramdani, A. Ibenbrahim, and D. Ben Sari (1996), Three dimensional upper mantle structure beneath the intraplate Atlas and interplate Rif mountains of Morocco, *J. Geophys. Res.*, *101*, 325–338.
Sébrier, M., L. Siame, E. M. Zouine, T. Winter, Y. Missenard, and P. Leturmy (2006), Active tectonics in the Moroccan High Atlas, *Comp. Rend. Geosci.*, *338*, 65–79.
Tadili, B., M. Ramdani, D. Ben Sari, K. Chapochnikov, and A. Bellot (1986), Structure de la croûte dans le nord du Maroc, *Ann. Geophys.*, *4*, 99–104.
Teixell, A. (1998), Crustal structure and orogenic material budget in the west central Pyrenees, *Tectonics*, *17*, 395–416.
Teixell, A., M. L. Arboleya, M. Julivert, and M. Charroud (2003), Tectonic shortening and topography in the central High Atlas (Morocco), *Tectonics*, *22*(5), 1051, doi:10.1029/2002TC001460.
Teixell, A., P. Ayarza, H. Zeyen, M. Fernández, and M. L. Arboleya (2005), Effects of mantle upwelling in a compressional setting: The Atlas Mountains of Morocco, *Terra Nova*, *17*, 456–461.
Teixell, A., P. Ayarza, E. Tesón, J. Babault, F. Alvarez-Lobato, M. Charroud, M. Julivert, L. Barbero, M. Amrhar, and M. L. Arboleya (2007), Geodinámica de las cordilleras del Alto y Medio Atlas: Síntesis de los conocimientos actuales, *Rev. Soc. Geol. España*, *20*, 119–135.
Van der Meijde, M., S. Van der Lee, and D. Giardini (2003), Crustal structure beneath broad-band seismic stations in the Mediterranean region, *Geophys. J. Int.*, *152*, 729–739.
Wigger, P., G. Asch, P. Giese, W.-D. Heinsohn, S.O. El Alami, and F. Ramdani (1992), Crustal structure along a traverse across the Middle and High Atlas mountains derived from seismic refraction studies, *Geol. Rundsch.*, *81*, 237–249.
Zelt, C., and R. Smith (1992), Seismic traveltime inversion for 2-D crustal velocity structure, *Geophys. J. Int.*, *108*, 16–34.
Zeyen, H., P. Ayarza, M. Fernandez, and A. Rimi (2005), Lithospheric structure under the western African-European plate boundary: A transect across the Atlas Mountains and the Gulf of Cadiz, *Tectonics*, *24*, 1–16.